The paper was published in the proceedings of the 7th International Conference on Earthquake Geotechnical Engineering and was edited by Francesco Silvestri, Nicola Moraci and Susanna Antonielli. The conference was held in Rome, Italy, 17 – 20 June 2019.

Earthquake Geotechnical Engineering for Protection and Development of Environment and Constructions – Silvestri & Moraci (Eds)
© 2019 Associazione Geotecnica Italiana, Rome, Italy, ISBN 978-0-367-14328-2

The shaking table with laminar box of the University of Messina

V. Bandini, E. Cascone, G. Biondi, G. Di Filippo, S. Ingegneri, O. Casablanca, D. Aliberti & F. Genovese
Department of Engineering, University of Messina, Italy

ABSTRACT: A new shaking table apparatus has been set up in the laboratory EUROLAB-CERISI of the University of Messina (Italy), consisting of a shaking table, a large laminar box and an automated system for soil deposition. A servo-hydraulic actuator can excite the shaking table in one direction reproducing both real and artificial seismic motions. A 6m-long, 1.5m-wide and 2m-high laminar box has been assembled to replicate the plane strain conditions. The soil deposition system consists of a hopper that can be moved above the soil container. The velocity of the hopper, the width of its lower opening and the soil falling height can be adjusted to attain the desired relative density in the soil model. The paper provides details of this experimental facility and describes the results of static tests, aimed to demonstrate that plane strain conditions are actually verified, as well as of dynamic tests, aimed to characterize the performance of the equipment.

1 INTRODUCTION

Research in earthquake geotechnical engineering and numerical modelling of the dynamic response of geotechnical systems has shown considerable development in the recent past. The use of sophisticated tools for numerical analysis requires a sound understanding of the dynamic behaviour of the soil, of soil structure interaction (SSI) and phenomena related to propagation of seismic waves in soil deposits, such as site amplification and liquefaction. Understanding of soil response to dynamic loading and validation of numerical analyses can be achieved by means of tests on physical models reproducing the desired geotechnical scheme. Physical modelling allows studying the response of complex geotechnical systems under laboratory-controlled conditions by simulating loading conditions that can hardly be monitored in real systems.

Typically, seismic tests on scaled models are performed either under normal gravity conditions, using shaking tables, or under an augmented gravity field, in a centrifuge. In shaking table tests of reduced scale models, the similitude requirements in terms of stress and strain against the prototype cannot be satisfied so typically they are used to investigate simple patterns of behaviour and to understand the basic mechanisms of system failures. Recently, large-scale shear devices were constructed to overcome some limitations of the more conventional small containers and allow better reproducing the prototype field conditions; moreover, in a large soil container the boundary effects have a minor influence on the model response and the volume of soil situated in the central part of the container is able to mimic with reasonable approximation the prototype field conditions.

Different types of soil containers are available worldwide (i.e. rigid containers, flexible containers, active boundary containers, equivalent shear beam containers) mounted on shaking tables that differ for shape, dimensions and performance (i.e. displacement capacity, degrees of freedoms, maximum payload); details of some geotechnical shaking table facilities available in European laboratories are summarized in Table 1 where L, W and H represent the length, width and height of the soil container, d_{max} and P_{max} are the maximum displacement amplitude and payload of the shaking table.

Table 1. Examples of European shaking table facilities.

Institution	L (m)	W (m)	H (m)	L/H	d_{max} (mm)	P_{max} (ton)	Reference
EUROLAB - Messina	6	1.5	2	3.0	±255	32	Ricciardi & Cascone 2015
EQUALS- Bristol	4.8	1	1.15	4.8	±150	15	Wood et al. 2002
LNEC - Lisbon	2	0.75	1.75	1.1	±175	40	Carvalho et al. 2010
IZIIS- Skopje	2	1	1.5	2.0	±125	40	Bojadjieva et al. 2014
Bogazici University	0.9	0.9	1.65	0.5	±120	10	Cengiz & Güler 2017
CEDEX- Madrid	3	1.1	1.2	2.7	±100	10	Estaire 2007

Rigid containers, extensively used in the 1980's, are nowadays overcome as they do not allow the soil specimen to deform uniformly, inhibit the development of large shear strains and trap energy through wave reflection. As a consequence, the use of a laminar shear box to house the soil specimen has become a common practice since it allows the soil model to deform under seismic loading in the same manner as in the prototype condition (Gibson 1997; Prasad et al. 2004; Ueng et al. 2006; Biondi et al. 2003, 2015).

This paper provides preliminary details of a new experimental facility, set up in the EUROLAB-CERISI laboratory of the University of Messina, pointing out that the plane strain conditions are actually verified during the filling procedure and focusing on the performance of the large-scale laminar box and on the capability of the servo-hydraulic control system to reproduce a prescribed acceleration time-history at the shaking table platform. Further data about the performance of the facility can be found in the paper by Cascone et al. (2019).

2 EXPERIMENTAL EQUIPMENT

The laboratory EUROLAB-CERISI of the University of Messina houses a large single degree of freedom shaking table equipped with a large-scale laminar box for testing physical models of geotechnical systems under seismic loading conditions (Figure 1). Bosch-Rexroth company designed and manufactured the whole equipment. The laminar box is a large rectangular flexible soil container with internal length L= 6 m, width W= 1.5 m and height H= 2 m (Table 1).

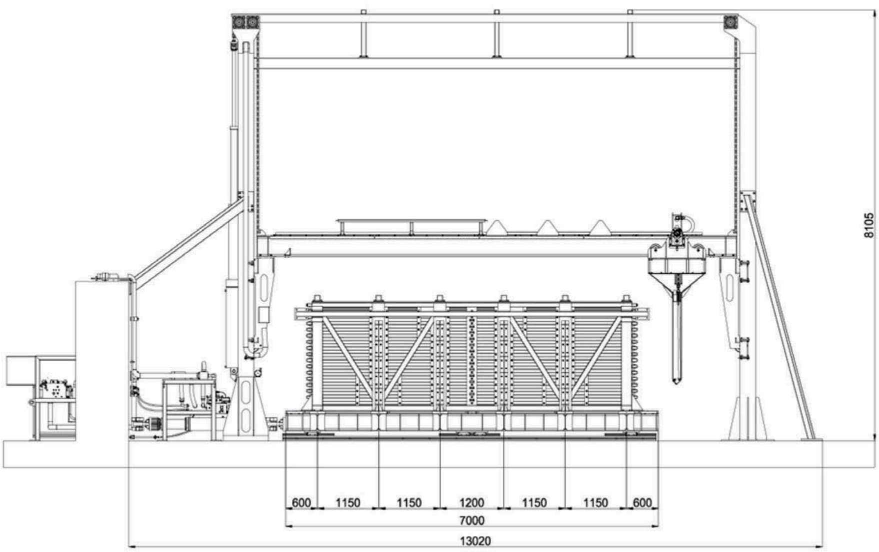

Figure 1. A scheme of the EUROLAB equipment for shaking table tests on geotechnical system.

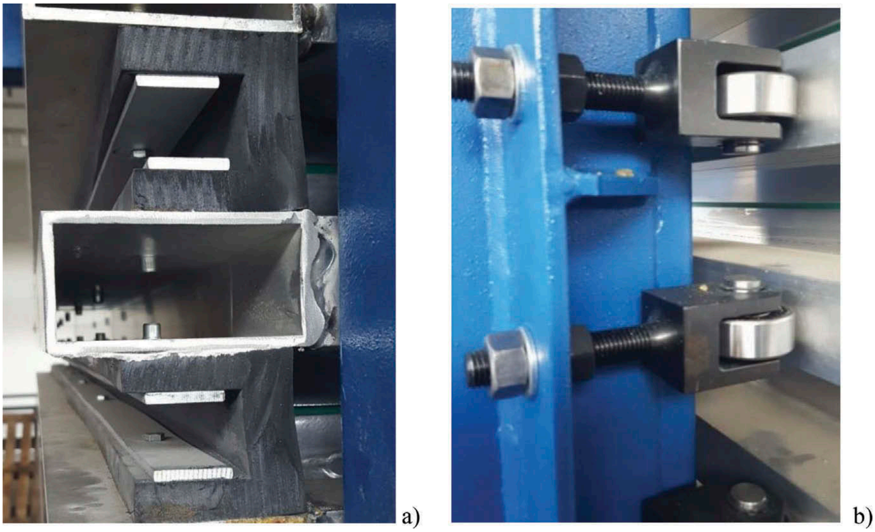

Figure 2. Details of the laminar box: a) aluminium rectangular hollow section rings and rubber sections, b) steel wheels (polyzene sheet is visible between two aluminium rings).

The most important advantage of a large-scale shear device is that the prototype-to-model linear scale ratio may be kept reasonably low and the model can be excited with dynamic loading capable of inducing inertial forces comparable to those induced by real earthquakes. The laminar box consists of 18 aluminium rectangular hollow section rings, which are stacked alternately with rubber sections (Figure 2a). The rings and their supporting system provide lateral confinement of the soil in order to reproduce zero lateral deformation conditions (k_0 conditions), while the EPDM (Ethylene-Propylene Diene Monomer) rubber layers and the polyzene sheets allow the container to deform under horizontal shaking according to a shear beam mode, reproducing as far as possible, a free-field condition. The aluminium alloy is adopted for its strength and stiffness to provide unyielding boundaries, and for its light weight to minimize the effect of inertia of the shear box on the soil movements. The floor of the laminar box is covered with a sheet of abrasive paper to aid the transmission of shear waves; the internal end walls are similarly treated to enable generation of complementary shear stresses. The internal lateral walls are covered two layers sheets lubricated with hexagonal boron nitride. This arrangement allows minimizing the friction between the internal side of the lateral walls and the soil specimen.

The laminar box is transversally restrained by a rigid steel frame and a system of steel roller bearings to provide adequate stiffness against lateral deformations and constrain the motion in the longitudinal direction (Figure 2b), preventing unwanted torsional movement of the container during shaking.

The stack is secured to the shaking table by its base and shaken horizontally lengthways by a servo-hydraulic actuator with ±255 mm stroke and 32 tonnes of payload. Hydraulic power for the actuator is provided by three hydraulic pumps capable of delivering 1200 litre/min at a working pressure of 300 bar. Linear guideways consisting of sliding rails and bearing blocks are used to allow an almost frictionless horizontal movement without vertical motions.

A pluviator was designed for preparing the soil specimen inside the laminar box by the pluviation method. The spreader consists of a hopper, with an internal volume of 1.5 m^3, attached to a supporting frame; the hopper can move back and forth above the soil container at constant velocity (1-10 cm/s), driven by a stepper motor, and the direction of the motion is automatically reversed inside specific limit conditions measured by proximity sensors. The soil falls from a rectangular opening located at the bottom of the hopper; the opening width can be varied from 1mm to 15 mm. The beam supporting the hopper can also move up and down allowing to adjust the drop height for the falling soil particles in the range 30-3000 mm from the soil level

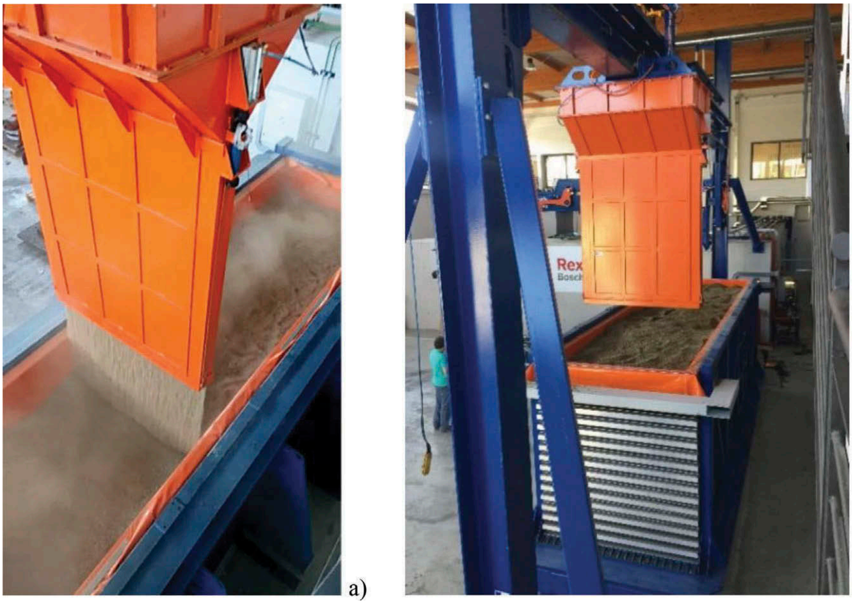

Figure 3. A typical deposition stage configuration.

inside the laminar box. The capability of the described pluviation system to control the velocity of the hopper, its opening width and the drop height allows achieving a high degree of spatial uniformity both in terms of relative density and grain size distribution of the soil model inside the laminar box. Figure 3 shows the pluviation system during a typical deposition stage.

3 DEFORMABILITY OF THE LAMINAR BOX DURING FILLING

To evaluate the deformability of the side walls of the laminar box, a series of measurements along the height of the walls at different stages of filling were performed. A laser tracker system (Leica AT930) has been used to measure the coordinates of 56 points on the side walls (28 for each side) and 26 points on the shaking table platform. The majority of the monitored points was concentrated in the central part of the sidewalls of the laminar box as it experienced the maximum deformations during filling stages. Figure 4 shows the location of the monitored points along one of the side walls (denoted as SX).

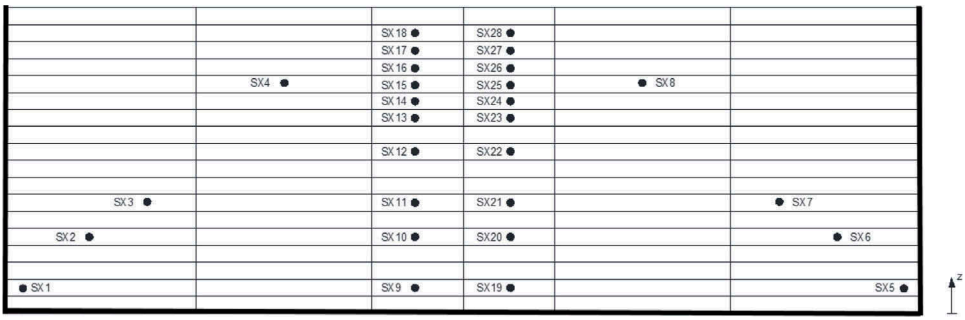

Figure 4. Location of the monitored points along one of the side walls (SX) of the laminar box.

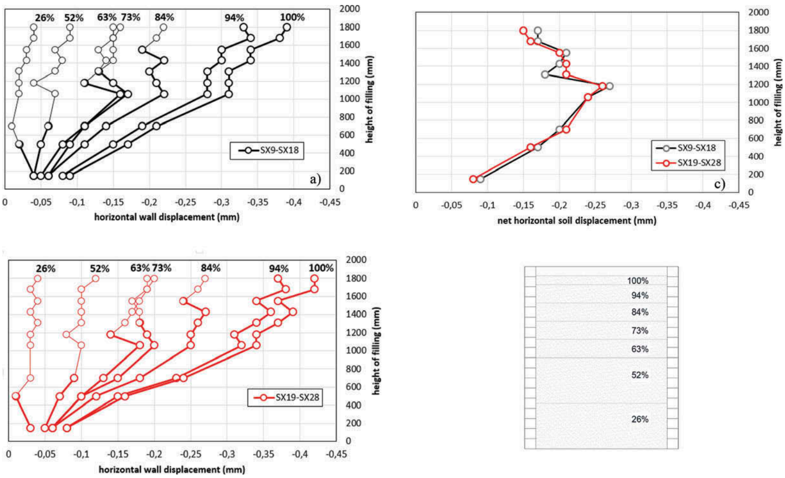

Figure 5. Cumulated horizontal displacement on the left side wall of the laminar box during the filling process: a) SX9-SX18, b) SX19-SX28 and c) net horizontal soil displacements for a filling ratio of 100%.

The container was filled with a natural dry sand (D_{50}=1.5 mm); the sand-filling process was carried out in seven steps up to a final height of 1910 mm. At the first step sand was poured into the box up to a height of 500 mm, corresponding to a filling ratio of 26%; in the following steps the height of the sand was raised to 1000 mm (52%), 1200 mm (63%), 1400 mm (73%), 1600 mm (84%), 1800 mm (94%) and 1910 mm (100%). Figure 5 shows the results of the measurements in terms of cumulated horizontal displacement of the points located along the central part of the left side wall of the laminar box (i.e. points SX9-SX28). As it is shown in Figures 5a and 5b relative to the side wall SX, the deflections of the wall progressively increased from the bottom to the top of the container while increasing the height of the sand; the effect of horizontal earth pressures on the wall deformation was observed both in the portion of the wall in contact with the infilled sand (thick lines in Figure 5a,b) and in the upper free empty part (thin lines). At the end of filling a maximum wall displacement of 0.405 mm, evaluated averaging measurements taken at points SX18 and SX28, was reached at the top of the container.

To evaluate the actual horizontal displacement of the soil relative to the wall, the net horizontal displacement was calculated for each point subtracting, from the cumulated displacement, the amount measured until the sand had not reached the height of the considered point. Figure 5c shows the distribution of soil displacements behind the wall considering the deformations of the wall during each stage of filling. At 100% of filling (H=1910 mm), the soil behind the wall experienced a maximum displacement of 0.265 mm (mean value of measurements taken at points SX13 and SX23) at a distance of 1200 mm from the bottom of the container. As a result, the maximum lateral displacement experienced by the soil specimen during the filling procedure is about $0.14 \cdot H/1000$ which is more that an order of magnitude lower than the displacement required to attain the active limit state in sands (Clough & Duncan, 1991).

4 PERFORMANCE OF THE SHAKING TABLE DURING DYNAMIC TESTS

Large servo-hydraulic shaking tables such as that available at the EUROLAB laboratory of the University of Messina are complex systems designed to subject large geotechnical specimens to extreme seismic loads. The severity of the earthquake ground motions that has to be reproduced by the shaking table systems and the size of the specimen inside the laminar box that has to be shaken required the implementation of a robust controller to guide the table in following a prescribed motion.

The servo-hydraulic control system operates in displacement control mode. A displacement feedback loop is used to control the motion of the table and a force stabilization is provided by an additional actuator force feedback loop which concurs to damp out the oil column resonance. As the key element in shaking table tests is the capability of the system to accurately reproduce prescribed acceleration records which are usually broadband signals, the displacement control strategy has been enhanced with additional feedforward control signals in order to increase the fidelity in acceleration reproduction. Then to optimize the signal reproduction capability a "tuned" shaking table control system was implemented in which a total transfer function is applied between the command and feedback signals characterized by a unit gain and zero phase shift across the entire operating frequency range under loaded table conditions. Since there may be dynamic interactions between the specimen and the table, the tuning process has been conducted with the specimen mounted on the table, as suggested by Luco et al. (2010).

In order to verify the capability of the "tuning" process implemented in the control system, a set of different acceleration records was selected from ITACA and PEER seismic databases (Luzi 2017; Ancheta et al 2013); these accelerograms were double integrated to derive the displacement time-histories to apply as command signals to the servo-hydraulic actuator system. For the selected records Table 2 lists the values of the moment magnitude M_w of the seismic event, the Jooner & Boore distance R_{jb} of the seismic station, the peak acceleration a_{max}, the mean period T_m, the Arias intensity I_a and the number of equivalent loading cycles N_{eq} evaluated according to the procedure by Biondi et al. (2012). Data in Table 2 show that the selected accelerograms span over wide ranges of amplitude, frequency and energy content.

The tests were carried out imposing the displacement time-histories to the shaking table and an accelerometer of high output capacitance, operating over a frequency range of 0 - 3000 Hz, was used to record the acceleration of the table. To reduce noise, signals from the instrument were passed through a low pass Butterworth filter set to 100 Hz; data were acquired at a sampling rate of 1000 Hz.

Measured acceleration time-histories were then compared to the target seismic acceleration records and the relative error ε_a on the peak acceleration, as well as the relative root mean square error ε on the constant ductility displacement (ε_{SD}) and acceleration spectrum (ε_{SA}) and on the Fourier amplitude spectrum (ε_F) were evaluated using the following equations:

$$\varepsilon_a = \frac{a_{ref} - a_m}{a_{ref}} \tag{1}$$

$$\varepsilon = \frac{\sqrt{\sum_{i=1}^{N} \left(x_{ref,i} - x_{m,i}\right)^2}}{\sqrt{\sum_{i=1}^{N} \left(x_{ref,i}\right)^2}} \tag{2}$$

In equation 1 a_{ref} is the peak acceleration of the target motion while a_m is the peak acceleration measured at the table; analogously, in equation 2 x_{ref} and x_m are the target spectral

Table 2. Characteristics of the acceleration time-histories used in the dynamic tests.

Earthquake	Station – Orientation Instrument	M_w	R_{jb} (km)	a_{max} (g)	T_m (s)	I_a (cm/s)	N_{eq}
Irpinia (1980)	Bisaccia – (North-South)	6.90	17.98	0.10	0.62	28.53	11.39
Kobe (1995)	Kobe University – (090)	6.90	0.92	0.31	0.38	81.73	5.90
Loma Prieta (1989)	Gilroy Array #1- (090)	6.93	9.64	0.49	0.27	169.00	7.59
Northridge-01 (1994)	LA-Wonderland Ave – (185)	6.69	20.29	0.16	0.26	20.40	8.02
San Fernando (1971)	Pasadena-Old Seismo Lab- (270)	6.61	21.50	0.21	0.24	34.21	9.02
Sicily (1990)	Sortino – (East-West)	5.60	24.58	0.11	0.15	5.52	5.33
Umbria Marche (1997)	Cesi Monte –(North-South)	5.60	6.20	0.18	0.18	11.41	4.74
Friuli (1976)	Tolmezzo – (East-West)	6.40	10.22	0.32	0.37	120.55	9.70

Table 3. Comparison between target and measured acceleration time-histories: relative errors.

Record	ε_a	ε_{SD}	ε_{SA}	ε_F
Bisaccia – (North-South)	50%	14%	13%	38%
Kobe University – (090)	11%	9%	9%	30%
Gilroy Array #1- (090)	12%	13%	7%	24%
LA-Wonderland Ave – (185)	33%	22%	19%	43%
Pasadena-Old Seismo Lab- (270)	15%	28%	19%	42%
Sortino – (East-West)	9%	17%	21%	55%
Cesi Monte –(North-South)	35%	19%	39%	58%
Tolmezzo – (East-West)	12%	12%	11%	23%

datum and the corresponding datum evaluated using the measured motion, respectively, while N is the number of datapoints describing a given period interval. The errors evaluated for the all tests carried out are reported in Table 3.

Apart from a few cases, relative error on peak acceleration is generally lower than 15%, relative error on the displacement and acceleration spectra is generally less than 30%, while relative error on Fourier amplitude spectra (ε_F) is generally less than 50% and is affected by differences between measured and target motion at high frequencies.

To get an overview of the performance of the "tuned" servo-hydraulic control system in terms of fidelity in signal reproduction, the target and the measured acceleration time-histories were compared for each test.

In Figure 6 the comparison relative to the Tolmezzo accelerogram is shown. It can be observed that the measured acceleration time-history reproduces satisfactorily the real accelerogram (Figure 6 a) but exhibits some amplification in the strong motion peaks. The computed 5% damping acceleration spectra (Figure 6b) and the Fourier amplitude Spectra (FAS, Figure 6c) point out that the differences between the target and measured motions can be observed predominantly in the high frequency range that are far from the principal frequency of the target accelerogram. The Amplification Function obtained by the ratio between the *FAS* of

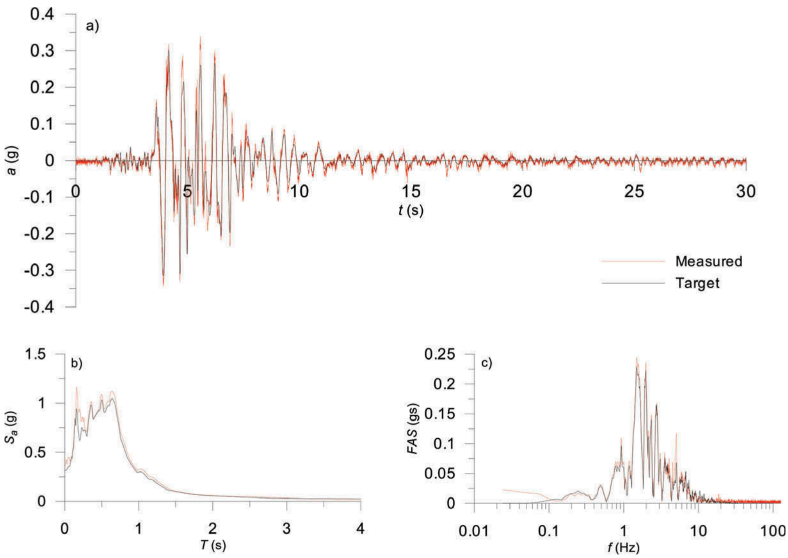

Figure 6. Comparison between target and measured motions for the case of the Tolmezzo accelerogram: a) acceleration time-histories, b) Acceleration spectra and c) Fourier amplitude spectra.

the measured and the target accelerogram resulted close to unity over the frequency range 0-4 Hz, that includes the predominant frequency of the Tolmezzo accelerogram (f=1.49 Hz).

5 CONCLUDING REMARKS

In this paper a description of the new equipment for dynamic physical modelling of geotechnical systems housed in the EUROLAB Laboratory of the University of Messina is provided, giving details of the geometry and the mechanical features of the shaking table and of the laminar box. The results of static tests carried out measuring the wall container displacements during sand filling stages proved that plane strain conditions are verified with good accuracy. The dynamic tests gave an overview of the equipment performance highlighting the capability of the shaking table to reproduce the desired acceleration input. Relative errors evaluated between measured and target motions for a set of accelerograms resulted reasonably acceptable since they are mostly affected by the equipment response at frequencies typically higher than the input motion frequency.

REFERENCES

Ancheta T.D., Darragh R.B., Stewart J.P., Seyhan E., Silva W.J., Chiou B.S.J., Wooddell K.E., Graves R.W., Kottke A.R., Boore D.M., Kishida T., Donahue J.L. 2013. PEER 2013/03 – PEER NGA-West2 Database.

Biondi G., Massimino M.R., Maugeri M., Taylor C. 2003. Influence of input motion characteristics on dynamic soil-structure interaction by shaking table tests. WIT Transactions on the Built Environment, (72), 2003: 225-234.

Biondi G., Cascone E., Di Filippo G. 2012. Affidabilità di alcune correlazioni empiriche per la stima del numero di cicli di carico equivalente, *Rivista Italiana di Geotecnica*, 46 (2), 9-39.

Biondi G., Massimino M. R., Maugeri M. 2015. Experimental study in the shaking table of the input motion characteristics in the dynamic SSI of a SDOF model. *Bulletin of Earthquake Engineering*, 13(6),1835-1869.

Bojadjieva J., Sesov V., Edip K., Gjorgiev I. 2014. Some important aspects in experimental setup for liquefaction studies on shaking table tests. *2nd Eur. Conf. Earthquake Engineering and Seismology*.

Carvalho A.T., Bile Serra J., Oliveira F., Morais P., Ribeiro A.R., Santos Pereira C. 2010. Design of experimental setup for 1 g seismic load tests on anchored retaining walls. *Physical modelling in geotechnics*. Taylor and Francis Group, London.

Cascone E., Aliberti D., Bandini V., Biondi G., Casablanca O., Di Filippo G., Ingegneri S., Genovese F. 2019. A new shaking table apparatus for large scale physical modelling of geotechnical systems. *XVII ECSMGE-2019*, Reykjavic.

Cenzin C & Guler E 2017. Design of a Novel Laminar Box for evaluating the seismic Performance of Soils. *6th International Young Geotechnical Engineers' Conference (iYGEC6)*.

Clough, G. W., J. M. Duncan. 1991. Earth pressures. *Foundation engineering handbook*. Springer, Boston, MA, 1991. 223-235.

Estaire J. 2007. Shaking table tests on shallow foundations. *WIT Transactions on the Built Environment*.

Gibson, A.D. 1997. Physical scale modelling of geotechnical structures at one-g. *PhD thesis*, California Institute of Technology, Pasadena.

Luco J.E., Ozcelik O., Conte J.P. 2010. Acceleration tracking performance of the UCSD-NEEDS Shake Table. *Journal of Structural Engineering*, 136 (5): 481-490.

Luzi L., Pacor F., Puglia R. 2017. Italian accelerometric archive v 2.2. *Istituto Nazionale di Geofisica e Vulcanologia, Dipartimento della Protezione Civile Nazionale*, 10.13127/ITACA.2.2.

Prasad S.K., Towhata I., Chandradhara G.P., Nanjundaswamy P. 2004. Shaking table tests in earthquake geotechnical engineering. *Curr Sci* 87(10):1398–1404.

Ricciardi G., Cascone E. 2015. Il nuovo laboratorio EUROLAB del Centro di eccellenza Ricerca e Innovazione per Strutture ed Infrastrutture di grandi dimensioni (CERISI). *XXI Secolo – Scienza e Tecnologia*, 3: 29-36.

Ueng T.S., Wang M.H., Chen M.H., Chen C.H., Peng L.H. 2006. A Large Biaxial Shear Box for Shaking Table Test on Saturated Sand, *Geotechnical Testing Journal*, 29(1): 1-8.

Wood D.M., Crewe A., Taylor C. 2002. Shaking table testing of geotechnical models. *International Journal of Physical Modelling in Geotechnics*, 1: 1-13.